Light Metals 2011 *Edited by: Stephen J. Lindsay*
TMS (The Minerals, Metals & Materials Society), 2011

INFLUENCE OF TECHNOLOGICAL AND CONSTRUCTIVE PARAMETERS ON THE INTEGRITY OF THE BOTTOM OF ALUMINUM REDUCTION CELLS DURING FLAME PREHEATING

Alexander Arkhipov, Gennadiy Arkhipov, Vitaliy Pingin
RUSAL Engineering & Technological Centre LLC, Pogranichnikov str. 37 bild. 1, Krasnoyarsk, 660111, Russia

Keywords: preheating, mathematical modeling, ANSYS, CFD, cell life.

Abstract

The effects of preheating technology, cathode block materials and other factors on the integrity of the cell during flame preheating of aluminum reduction cells were investigated. The temperature fields, gas dynamics, and stress-strained state of the reduction cell during flame preheating were studied using mathematical modeling in an ANSYS finite-element package and Star-CD CFD-package. The best way to cover the peripheral seams during preheating has been identified.

Introduction

The main cause of premature failure of an aluminum reduction cell is the violation of the integrity of the bottom and, as a consequence, the leakage of the melt to the collector bar and into the base of the cathode. One of the main factors affecting the integrity of the bottom (25%, according to the literature [1]) is the technology of preheating and startup of the reduction cell. The goal of this work was to analyze the effect of technology of flame preheating on the integrity of the bottom and to select the optimal parameters for its performance on the basis of mathematical modeling. To achieve this goal, it is necessary to solve a set of equations of heat and mass transfer and fuel combustion, thermal conductivity, and the mechanics of a deformed solid body [2, 3]. Their analytical solution is inapplicable to reduction cell preheating; therefore, to calculate the temperature fields of the latter, we used a STAR_CD program based on the control volume method; and to calculate the stress-strained state (SSS) of the cathode we used an ANSYS finite element program.

Computational procedure

The procedure for calculating the temperature field of the reduction cell and the stressed-strained state of the cathode, as well as the results of an analysis and the results of their correspondence to the criteria of high quality preheating, involves the following:

(i) The development of a three-dimensional computer model by the drawings and production flow sheet of preheating, which repeats the geometry of the operating or designed reduction cell and gas-air medium (Fig. 1).

(ii) The specification of necessary initial and boundary conditions.

- For the gas-air medium, these are the reaction of fuel combustion

$$C_7H_{16} + 11O_2 \rightarrow 7CO_2 + 8H_2O \quad (1)$$

the velocity of output of the fuel and air from the burner and zero pressure in the orifices for the output of the gases through the cover material.

- For the problem of heat conductivity, these are the coefficients of heat exchange (allowing for emission) on free surfaces of the shell, the temperature of the surrounding medium, and the initial temperature of the cell.
- For the SSS these are the loads from the anode assembly and the limitation of displacements of the cathode assembly depending on the conditions of its mounting in the electrolysis shop.

(iii) The specification of the properties of materials and the gas-air medium, namely: density, heat conductivity, heat capacity, dynamic viscosity, elasticity modulus, the Poisson coefficient, yield point, and secant elasticity modulus (the temperature range under consideration for materials is from –40 to +1000°C).

(iv) Computations of the transient temperature field of the cell using a Star-CD program from the beginning to the end of preheating while allowing for fuel combustion and heat-and-mass transfer in a gas-air medium.

(v) An analysis of the temperature field for an evaluation of the correspondence to the calculated plot of the increasing temperature to the plot designed according to the process flowsheet of the preheating cell.

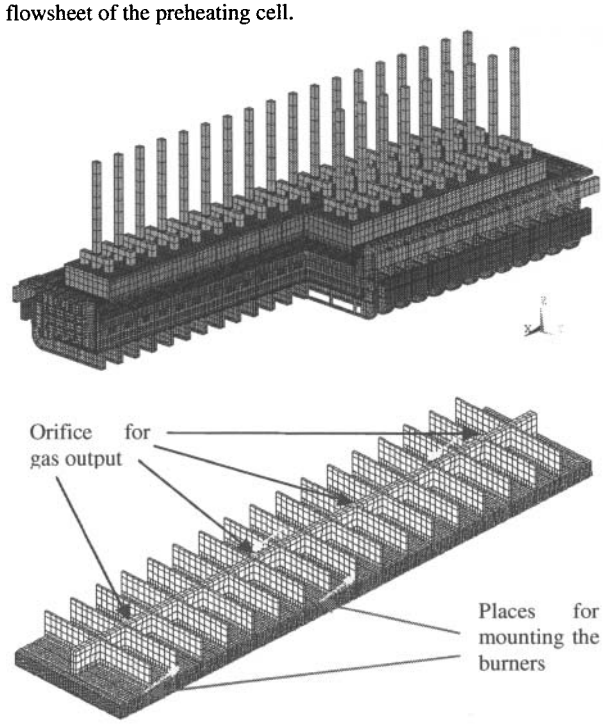

Figure 1. Finite volume model of the cell for a calculation of the flame preheating. (a) Solid state part and (b) gas-air part with places of mounting burners and outlets.

(vi) If necessary, a variation in the process parameters of preheating, lining design, and cover of the cell, as well as a repeated computation of the temperature field.

(vii) Transfer of the thermal field of the cell obtained in STAR_CD into the ANSYS program and the fulfillment of calculations of the stress-strained state of the cathode facility for different durations of preheating.

(viii) An analysis of the strains and mechanical stresses and evaluation of integrity of the bottom with the use of the strength criterion of its materials.

(ix) If necessary, a change in the process parameters of preheating, lining design, and covering of the cell, as well as repeated calculations of the temperature field and SSS.

(x) The development of recommendations for a change in the process parameters of preheating and/or design of the cathode assembly to provide the integrity of the bottom in the preheating process of the cell.

The computational procedure and preheating model of the cell were verified by a comparison of calculated and measured (embedding thermocouples into the lining and mounting displacement sensors) data on the temperature of the bottom surface, as well as the temperature and deformations of the cathode shell and lining.

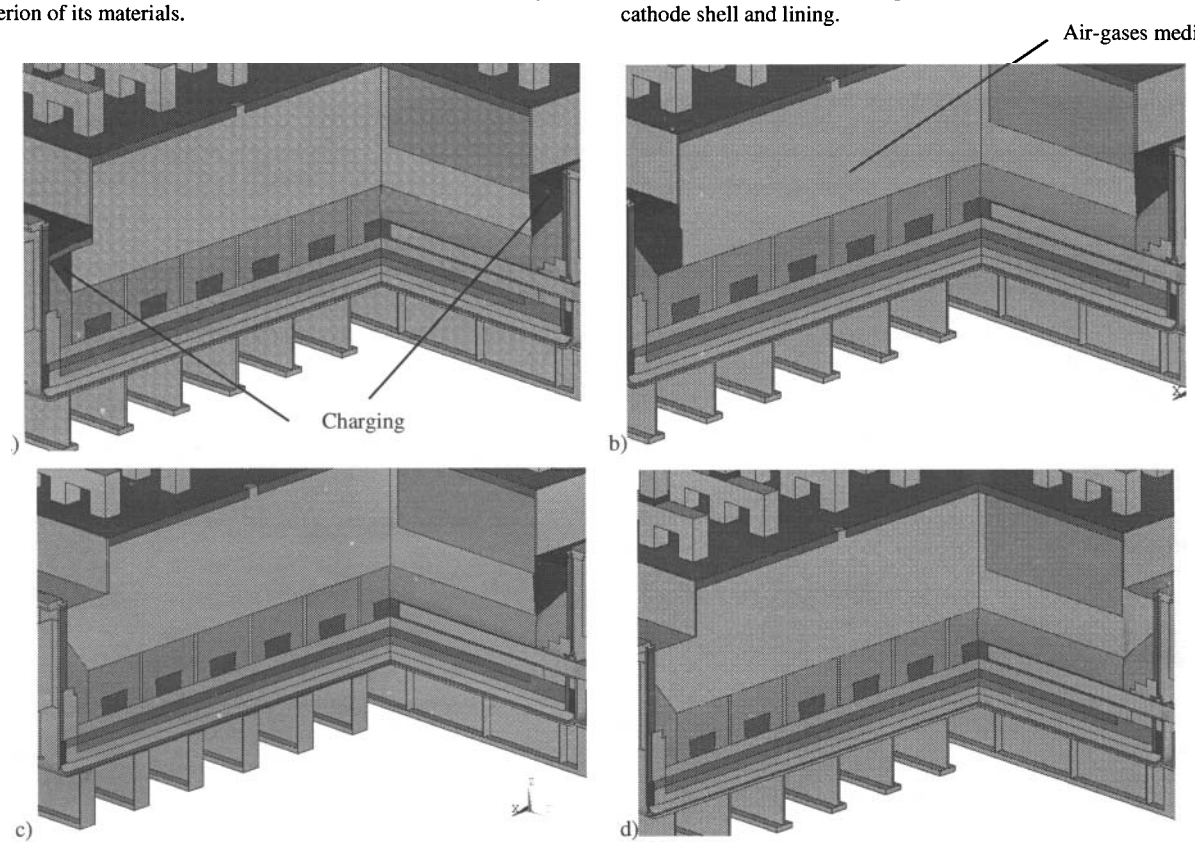

Figure 2. Variants 1–4 for a calculation of the flame preheating of the cell.

Results of calculations

The flame preheating of the cell for a current of 300 kA with prebaked anodes and a cradle cathode case was modeled. Cell was preheated by Hotwork diesel equipment with 4 burners pointed out on Figure 1b. The calculations of the following types of preheating and cell design were performed.

(1) The starting variant: the cell design has a 30% graphite content in cathode blocks (CB), the side–anode space (SAS) is completely charged with crushed recycled cryolite (CRC), and the end–anode space (EAS) is charged with CRC from silicon carbide plates to the boundary "end periphery seam–cathode block" (Fig. 2a). The preheating time is 64 h, and the fuel consumption is 6970 kg.
(2) Variant *1*, but the EAS is charged with CRC from silicon carbide plates to end anodes (Fig. 2b).
(3) Variant *1*, only the EAS is not charged with CRC but is covered with a heat-insulating plate from above (Fig. 2c).
(4) Variant *3*, only the SAS is not charged with CRC, but is covered by a heat-insulating plate from above (Fig. 2d).
(5) Variant *1*, but the CB contains 100% graphite.
(6) Variant 1, but the CBs are graphitized.

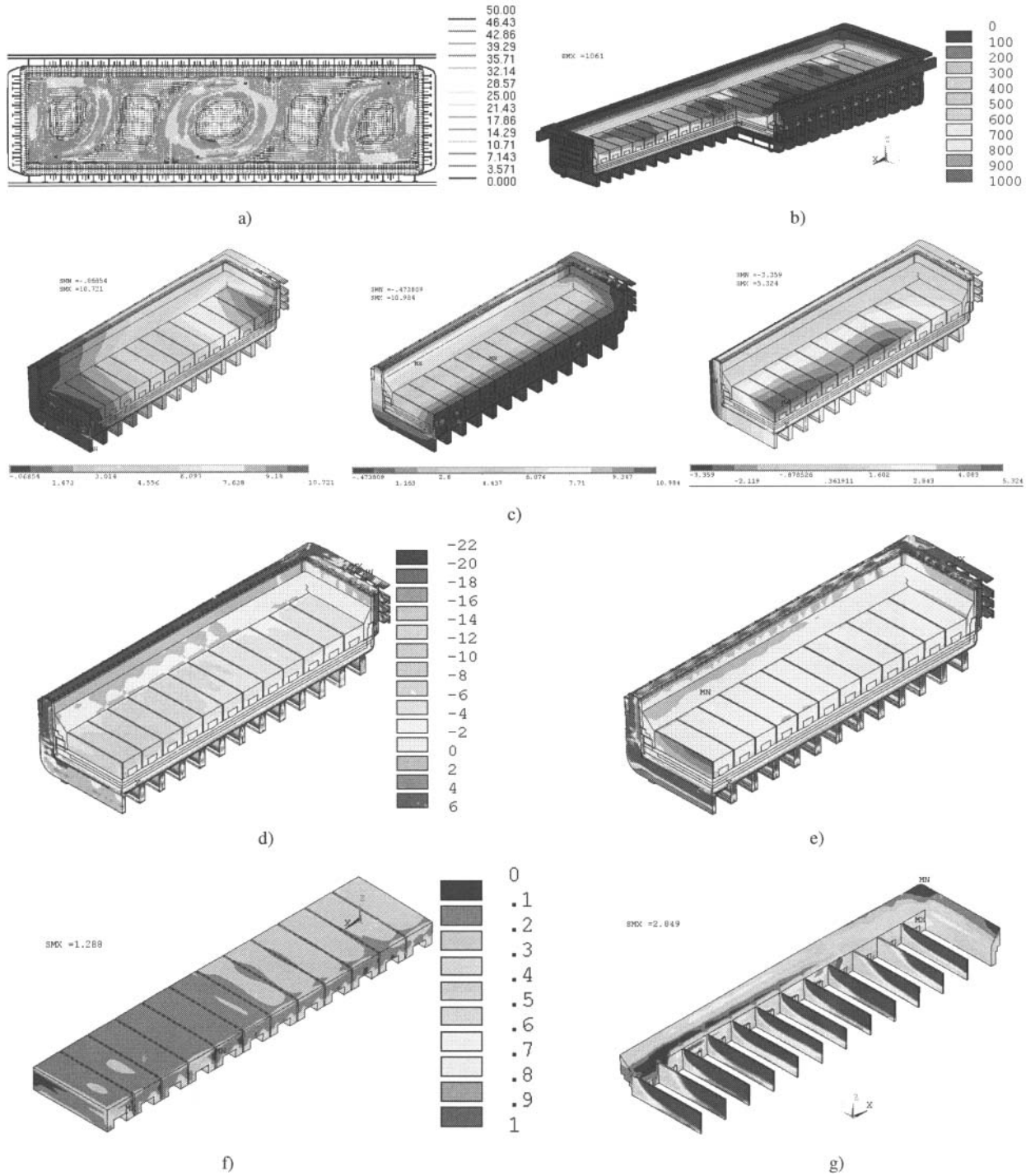

Figure 3. Results of a calculation of the flame preheating of the cell (Variant 1). (a) Velocity field in the gas_air medium; (b) temperature field of the cathode facility; (c) displacements of the cathode facility in the longitudinal, transverse, and vertical directions; (d, e) normal stresses in the longitudinal (d) and transverse (e) directions; and (g, f) the Gol'denblat–Kopnov strength criterion [7] for cathode blocks (f) and seams from the bottom mass (g) (white means the overestimation of the scale).

(7) Variant 1, but the preheating time is reduced to 50 h due to an increase in process intensity after 35 h. The rate of the temperature rise is increased from a factor of 1.5 at $\tau = 35$ h to a factor of 1.67 to the end of preheating compared with variant 1. The fuel consumption is 5715 kg.

The results of calculation of the field of velocities of the gas-air medium, temperature field, and the SSS of the cathode facility for variant 1 of preheating cells are presented in Figure 3. The results of calculation of the temperature field and SSS for other variants of preheating and cell designs are presented in Tables I and II. Their analysis showed the following.

Variant 1.
The average bottom temperature in the end of preheating is 892°C. For the interblock seams over the entire height, t > 600°C; i.e., for them, as well as the periphery seams near the cathode units, the temperature exceeds the temperature of the onset of coking the cathode paste (400°C). At distance above approximately 100 mm, the temperature is below 400 °C in the periphery seams.

Compression of the bottom in the longitudinal direction is sufficient to conserve its integrity, excluding the peripheral seam, in which tensile stresses up to 2 MPa appear. Compression of the bottom in the transverse direction is also sufficient to conserve its integrity, since tensile stresses are observed only in the interblock seams as well as in the edge cathode blocks (up to 1.2 MPa). The causes of the appearance of the latter are the high temperature gradient and the insufficient rigidity of the paste in the end peripheral seam. However, in this variant of flame preheating, tensile stresses to not reach values dangerous for bottom integrity.

Variant 2.
The complete charge of the EAS to the bottom surface of the end anodes leads to a considerable decrease in the temperature of the end periphery seams and end cathode blocks (by 140–300°C). As a result of an increase in temperature gradients and a decrease in the rigidity of end seams, tensile stresses at the edges of the cathode blocks substantially increase and the danger of violation of the integrity of the bottom appears.

Variant 3.
The complete absence of charging in the EAS (the EAS is only covered from above by an MKRKG_400 heat_insulating board or a similar material) leads to a decrease in the average temperature of the bottom surface when compared with variant 1 from 892 to 817°C because of a large heat loss through the side walls, which is indicated by a substantial increase in the temperature of end walls of the shell from 143 to 557°C. The temperature of the longitudinal seams and CBs at the boundary with them decreased by 20–40°C. The average temperature of end seams increased more than by 100°C.

An analysis of the SSS showed that, in this variant of preheating, the possibility of formation of the cracks in end CBs decreases, but the deformation of end walls of the shell increases and a large danger of appearance of longitudinal and transverse cracks in the end seams and the detachment of the top of end seams from the silicon carbide plates appears.

Variant 4.
The absence of charging into the EAS and SAS leads to a substantial increase in the temperature of the longitudinal and end shell walls, as well as the end and longitudinal peripheral seams with a decrease in the bottom temperature in general. An increase in the temperature of the longitudinal shell walls determines the larger extension of its upper part, which is indicated by considerable displacements of the ends (32.4 mm), a substantial lift of the bottom (86 mm), and the displacement of the edge cathode block by a factor of more than 2 compared to variant 1. Compression of the bottom considerably worsens, and the danger that the interblock seams will open appears.

Variant 5.
When using cathode blocks with graphite content of 100% instead of 30%, an increase in the average temperature of the bottom surface from 892 to 911°C is observed. The temperatures of the longitudinal and end peripheral seams and CBs on the boundary with them considerably increase because of the higher thermal conductivity of the CBs. The maximum temperatures of the longitudinal and end shell walls at the level of the bottom surface are elevated by 40°C.

Compared with variant 1, there is no noticeable improvement or worsening of the bottom SSS. Preheating according to variant 2 with CBs containing 100% graphite leads to a noticeable improvement of bottom compression due to an increase in the temperature of edge blocks; end periphery seams; and, consequently, to the weakening of the tensile stresses in them.

Variant 6.
The use of graphitized cathode blocks makes it possible to substantially increase the temperature of the cathode assembly, and it weakly affects the improvement of its SSS during preheating by variant 1; however, it promotes a decrease in or the exclusion of negative consequences of incorrect preheating technology, for example, by variant 2.

Variant 7.
Shortening the preheating time from 64 to 50 h due to an increase in the process intensity leads to a decrease in the average temperature of the bottom surface from 892 to 827°C. Bottom compression in the longitudinal and transverse sections is almost indistinguishable from variant 1. The periphery seams, in which the tensile stresses are practically absent, and edge CBs, where the tensile stresses decreased from 1.2 to 0.5 MPa (which is associated with the lower preheating temperature), are exceptions.

Conclusions

(i) Of all the preheating technologies we considered, the best is variant 1; in this case, the whole surface of the cathode blocks contacts with the gas_air medium and periphery seams are charged with recycled cryolite.

(ii) Charging the EAS to the anode edge leads to the partial insulation of end CBs from the gas_air medium, a larger temperature gradient in the edges of the blocks in the direction of the longitudinal axis of the bath, and a lower temperature of end peripheral seams, which causes large tensile stresses in the end blocks and can cause their destruction during preheating or after the startup of the cell.

(iii) The complete exclusion of charging into the EAS causes strong heating (up to 557°C) of the end wall of the cathode case and its considerable deformation. In connection with this, the danger of appearance of longitudinal cracks in end peripheral seams or their detachment from silicon carbide plates emerges.

(iv) With the complete exclusion of charging into the EAS and SAS, the strong overheating of end and longitudinal walls of the cathode case is observed, which is accompanied by their substantial bending and a lift of the bottom. This in turn leads to the danger that the interblock and peripheral seams will open.

(v) The use of graphitized and graphite CBs gives no valuable improvements in the conservation of integrity of the bottom with the correct preheating technology, but decreases the probability of negative consequences in the case of nonoptimal preheating technology.

(vi) Shortening the preheating time from 64 to 50 h with an increase in the rate that the temperature rises after 35 h does not lead to an increase in the danger that the integrity of the bottom will be violated at the end of preheating; however, it could be accompanied by a larger electrical voltage during startup because of the weaker heating of the bottom.

REFERENCES

1. Sorlie M. and Oye H., *Katody v alyuminievom elektrolizere* (Cathodes in Aluminum Cell), Krasnoyarsk: KGU, 1997.

2. Mikheev M.A. and Mikheeva I.M., *Osnovy Teploperedachi* (Principles of Heat Transfer), Moscow: Energiya, 1977.

3. Arkhipov G.V., Barantsev A.G., and Pingin V.V., Abstracts of Papers, *V Mezhdunarodnaya konferentsiya "Alyuminii Sibiri_99* (V Int. Conf. "Aluminum of Siberia_99"), Krasnoyarsk, KGU, 2000, p. 147.

4. Arkhipov A.G. and Polyakov P.V., in *Alyuminii Sibiri 2004: Sbornik nauchykh trudov* (Aluminum of Siberia 2004: Collected Articles), Krasnoyarsk: Bona Kompani, 2004, p. 149.

5. Arkhipov A.G. and Polyakov P.V., Abstracts of Papers, *4_ya konferentsiya pol'zovatelei programmnogo obespecheniya CAD_FEM GmbH* (4th Conf. of Users of CAD_FEM GmbH Software), Shadskii A.S., Ed., Moscow, Poligon, 2004, p. 323.

6. Arkhipov A.G., Polyakov P.V., Dekterev A.A., and Litvintsev K.Yu., in *Alyuminii Sibiri_2004: Sbornik nauchykh trudov* (Aluminum of Siberia_2004: Collected Articles), Krasnoyarsk: Bona Kompani, 2005, p. 9.

7. Gol'denblat I.I. and Kopnov V.A., *Kriterii prochnosti iplastichnosti konstruktsionnykh materialov* (Criteria of Strength and Plasticity of Construction Materials), Moscow: Mashinostroenie, 1968.

Table I. Results of temperature calculations during the preheating of the cell

Zone of cathode facility	t, °C, for variants						
	1	2	3	4	5	6	7
Bottom							
Bottom surface, t_{max}	1050	1011	969	932	1061	1055	998
Bottom surface, t_{av}	892	846	817	757	911	918	827
Lower surface of cathode blocks, t_{av}	639	606	586	595	795	831	527
Average cathode blocks values	792	767	736	679	891	912	720
Middle of the longitudinal wall (input/output side)							
Top of the cathode block at the boundary with the peripheral seam	626/ 656	633/ 613	630/ 597	820/ 624	757/ 794	739/ 725	581/ 599
Bottom of the cathode block at the boundary with the peripheral seam	453/ 472	467/ 453	465/ 430	609/ 605	690/ 707	729/ 715	376/ 386
Center of the peripheral seam	529/ 553	540/ 522	508/ 475	483/ 496	746/ 767	764/ 750	467/ 480
Average bulk values of longitudinal peripheral seams	344	332	331	586	465	499	306
Middle of the end wall (duct/tap end)							
Top of the cathode block at the boundary with the peripheral seam	568/ 576	300/ 294	813/ 706	639/ 599	701/ 712	823/ 797	575/ 576
Bottom of the cathode block at the boundary with the peripheral seam	458/ 464	331/ 328	550/ 460	407/ 411	670/ 679	779/ 755	400/ 400
Center of the peripheral seam	505/ 513	331/ 326	644/ 550	497/ 488	708/ 718	830/ 806	477/ 477
Average bulk temperature of the end peripheral seams	358	209	587	490	495	525	366
Maximum of the cathode shell walls							
Ends	143	77	557	437	182	187	165
Longitudinal	160	160	160	564	202	198	165

Table II. Results of the calculation of the SSS

Zone of the cathode facility	Variant no.						
	1	2	3	4	5	6	7
Displacement of the shell, mm							
Top of the end wall in the longitudinal direction	9,3	8,2	13,4	32,4	9,9	12,4	8,3
End wall at the level of the middle of the CB height in the longitudinal direction	8,7	7,7	8,32	13,7	9,7	12,2	7
Top of the longitudinal wall in the transverse direction	10,5	9,7	9,14	12	12,3	14,7	8,8
Bottom center in the direction Z	2,5	2,2	2,5	82,9	1,6	3,1	2,8
Bottom displacement, mm							
Top of the edge CB in the longitudinal direction	10,7	11,7	9	18,1	10,5	13,4	9
Longitudinal deflection of the edge CB	1,5	1,7	2	-0,3	1,3	1,9	1,3
End of the middle CB in the transverse direction	5,8	5,5	5,1	4,9	6,1	8,3	5,1
Center of the top of the bottom in the vertical direction	5,2	4,9	5,1	86	5	7,2	5
Normal stress, MPa							
Edge* of the CB in the transverse direction	1,2	6,3	-1,5	-1,0	0,7	-2	0,5
RP of the end seam in the transverse direction	0,8	0,1	2,9	1,2	1,0	1,8	0,63
Maximal value of the Gol'denblat–Kopnov strength criterion [7]							
Ramming paste	2,9	3,3	5,1	6,1	3,4	2,7	2,63
Carbon blocks	1,3	1,53	0,94	0,99	1,05	0,84	1,3
Edge of last carbon block	0,4	1,07	0,51	0,2	0,41	0,43	0,34

* Boundary of edge CBs and end peripheral seams.